5.3 Other programs

5.3.1 Methane (R.Keir, G.Rehder)

Background
Methane is a trace gas in the atmosphere, and its concentration has varied over time. Proxy measurements made in ice cores indicate that over the last 200 years, the atmospheric methane has risen from about 700 to 1800 ppb volume, and, on a percentage basis, the rise has accelerated during the last decades at a rate faster than the rise of atmospheric CO_2. As with other transient tracers such as tritium and chlorofluorocarbons, the changing atmospheric concentration should result in a time dependent net input/output of methane to the ocean, the signature of witch should be observable in recently formed deep waters.

In addition to the atmosphere, methane is also influenced by production and consumption within the ocean. In the upper ocean, methane appears to be generated slowly by some microbial process, judging from weak maximums that sometimes occur under the base of the mixed layer. In addition, at hydrothermal vents and cold seeps found on compressional margins, methane is released into the deep sea. Nevertheless, older deep waters generally appears to have quite low methane concentrations due to slow oxidative consumption.

Since the majority of the ocean´s deep water is produced in the northern Atlantic, it is an area where the changing atmospheric exchange should influence the distribution of methane most strongly. In conjunction with the program being carried out by the SFB 460, measurements of the distribution of dissolved methane and its $^{13}C/^{12}C$ isotope ratio were carried out on M39/2. The isotope measurements should provide an indication of the extent of the methane decrease in the water column that is due to oxidation, because this process consumes the lighter isotope preferentially. On the other hand, the carbon isotope ratio of methane in the atmosphere has remained nearly constant over time, and changes in the distribution due to varying atmospheric concentration should not strongly affect the isotope ratio in the ocean.

Surface Water pCH_4
Since deep waters are formed from surface waters, one needs to observe whether the atmosphere does indeed tightly control the methane concentration in the open ocean where this formation occurs. During the entire cruise, the partial pressure of methane in the surface layer of the ocean as well as in the atmosphere was surveyed. This was accomplished by pumping from 5 meters below the surface directly to a gas equilibrator located in the wet lab. A sample of the air recirculated in the equilibrator is periodically shunted into a gas chromatograph equipped with a flame-ionization detector. Both the methane and the CO_2 partial pressure were measured, the latter by catalytic conversion to methane. These measurements were also carried out continuously on air pumped from overtop the bridge into the wet lab. The apparatus provides a semi-continuous measurement of the partial pressures in the water every twenty minutes and atmospheric measurements every 40 minutes.

The methane partial pressure in the surface water was close to that of the atmosphere over the area covered by the cruise track. During the last section as warmer waters were encountered, the methane partial pressure of the surface became slightly supersaturated, by about 5%.

The CO_2 partial pressure measurements by gas chromatography followed closely those made by the IfM group using the infared detector. The CO_2 partial pressure was more variable than that of methane, but the surface water was always undersaturated relative to the atmosphere (see 5.1.1.3). Our measured atmospheric CO_2 concentrations agreed very well with those measured with the infared technique, but the pCO_2 values measured in the water by gas chromatography were systematically lower than obtained from the IfM equilibrator system, by two or three percent. The reason for the discrepancy is not known, and this will be investigated subsequently ashore.

Discrete CH_4 Measurements

In order to measure the dissolved methane in discrete samples from the hydrocasts, a new procedure for separating the gas phase from the water was employed. Water from the Niskin bottles is drawn into a 200 ml glass syringe without contact to the air. The syringe is then connected to an evacuated 500 ml bottle. As the water is drawn into this bottle from the syringe, most of the dissolved gas separates from the liquid phase. Altogether, 400 ml of water from 2 syringes is added to each bottle. The gas is now led into an evaculated burette by injecting a degassed brine into the bottom of the sample through a sidearm at atmospheric pressure. At this point, 1 ml of gas is extracted and injected into a gas chromatograph equipped with a flame ionization detector. The gas remaining in the burette is collected in an evaculated vial for isotopic analysis by mass spectrometry ashore. In addition to the gas samples, on a few stations separate water samples were collected in air free bottles, and these will be returned to the shore-based laboratory for carbon isotope analysis. The dissolved gas in these samples will be stripped using helium, and the trapped methane injected directly into the mass spectrometer. These isotope measurements will be compared to those on the already separated gas samples.

Preliminary results from M39/2

The calculation of the dissolved methane concentration from the measured data involves estimation of the total volume of all dissolved gases using nitrogen solubility in seawater, which requires temperature and salinity data, and the observed dissolved oxygen measurements. Thus, the final work up of our measurements will be conducted following the cruise.

The measured methane mole fraction in the gas phase gives a qualitative indication of the dissolved concentration in the water, since the total dissolved gas volume typically varies by about +/-10% in the northeastern Atlantic. As an example of results obtained so far, we show the vertical profiles of the methane concentration in the extracted gas at Stations 260, 262, 264 and 266 along sections F and G. Station 260 was taken directly over the rift valley of the Mid-Atlantic Ridge, just south of the Charlie Gibbs Fracture Zone. The other three stations lie progressively eastward of the ridge, reaching to the Porcupine Basin. The profiles illustrate that the vertical distribution of methane in the upper 2500 meters along this line remains relatively constant. Methane in the upper 500 to 600 m is relatively uniform at about saturation with the atmospheric partial pressure. The concentration decreases over the next 100 meters or so, and then remains fairly constant at a value somewhat less than that equivalent to the atmosphere over the 800 to 2000 m depth range.

In contrast, the deeper methane concentrations show a marked variation in their horizontal distribution. Below the rim of the rift valley, the methane concentration increases rapidly to values greater than found in the surface water. Evidently, hydrothermal venting is supplying a source to the waters within the valley, but overtop the rim, the deep circulation sweeps away the excess. Away from the ridge, in the eastern basin, the deepest waters contain quite low methane concentrations. This is apparently due to the fact that this water is relatively old, having a component of Antarctic Bottom Water that has found its way into the eastern basin through the Romanche Fracture in the Mid-Atlantic Ridge at the equator.

Preliminary results from M39/4
As for leg M39/2, the final work up of our measurements will be conducted following the cruise. However, the measured methane mole fraction in the gas phase gives a qualitative indication of the dissolved concentration in the water, since the total dissolved gas volume typically varies by about +/-10% in the northwestern Atlantic. The vertical distribution of this property is presented along 3 sections consisting of profiles 22-33, 34-57, and 88-103. As a preliminary observation, it appears that the pattern of these distributions is quite similar to those of chlorofluorocarbon and dissolved oxygen. This clearly indicates that water mass "age" or degree of ventilation with the atmosphere has an important influence on the methane concentration in relatively recently formed waters.

In regard to methane in the upper water column, the methane partial pressure in the surface water was consistently in equilibrium with the atmosphere over the most of the area covered by the equilibrator survey. A slight oversaturation occurred during the short transit over shelf waters (200 m depth) near Greenland. A preliminary indication from the station data indi-cates that the upper few hundred meters of the water column generally have concentrations equivalent to the atmospheric concentration. However, a subsurface maximum was found at about 54°N on the N-S section from Cape Farvel, indicative of production in the upper water column (Section profiles 34-57). The maximum is found at the top of the thermocline, at a depth of about 200 m.

5.3.2 Tritium/helium sampling program results from M39, legs 4 and 5 (H. Hildebrandt, M. Arnold, R.Bayer)

The preparation of the water samples obtained during M39 for analyses of the helium isotopes and the tritium content started soon after arrival of the samples at the Heidelberg laboratory. The procedure includes the quantitative extraction of helium from the water and transfer of the gases in a glass ampoule as well as storage of the degassed water for ingrowth of ^{3}He in a preconditioned glass bulb. The measurements are performed in a dedicated helium isotope mass spectrometer which is accessible for helium measurements of samples from M39 since January, 1998. Mass spectrometric tritium analyses may be performed after a sample storage time of typically six months and the high quality tritium data production will start in summer 1998. Nevertheless, a preview of the tritium distribution at selected positions was obtained in the meanwhile by our low-level counting facility (data precision lower than obtained from mass spectrometric measurements).

First results obtained from profiles taken along the WOCE WHP-A1/AR7 leg are shown in Figure 46 where the spatial and temporal evolution of the mean tracer content in the density range of Labrador Sea Water (LSW) is depicted. Evidently and principally according to the transient input and the radioactive decay of tritium the concentrations (upper panel of the figure) decreased since our last occupation of the leg in 1994, the same trend was observed between 1991 and 1994. The second panel attributes to the transient character and shows all the data points currently available normalized to a common date, i.e. start of 1991 (tritium concentrations are given as TU91); in this plot almost no temporal variability is visible. On the contrary the ^{3}He excess concentrations in LSW at least in the western part of the subpolar North Atlantic changed since 1994 (third panel, ^{3}He is presented in a delta notation giving the per cent deviation of the ^{3}He content of the samples from that of surface water in equilibrium with the atmosphere): in the Labrador Sea and in the Irminger Sea δ^3He increased from 2% to 3-4%, a feature that is probably related to the ventilation rate of LSW which, according to hydrographic observations, diminished since 1994. This is also visible from the lower panel of the figure which presents formally calculated tritium/^{3}He ages in the LSW: apparently the LSW ages obtained from the M39 cruise increased by about 3-4 years compared to the situation in 1994. Further measurements are in progress and a more detailed discussion of the tracer distribution and its variability will be performed as the data set growths.

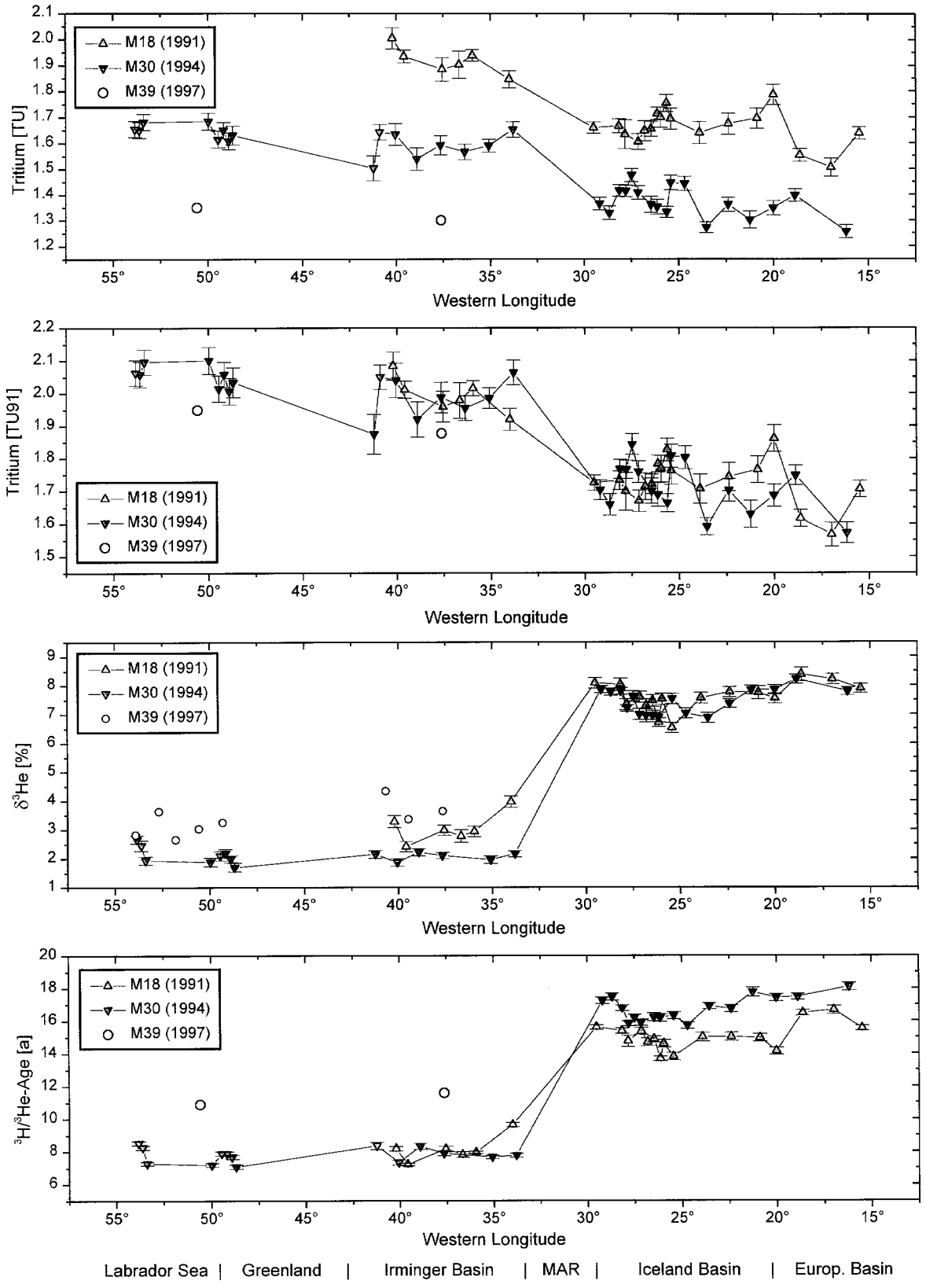

Fig. 46: Spatial and temporal evolution of tritium and delta ^{3}He in the density range of the Labrador Sea Water.

5.4. Paleoceanography

5.4.1 Water Column T-S Profiling (M. Huels, S. Jung, R. Zahn)

Methods
During METEOR cruise M39/1, a CTD/Rosette water sampler was deployed at 9 stations in water depths of 500-3500 m to obtain vertical temperature and salinity profiles as well as water samples. The Seabird Electronics CTD device consisted of supplementary oxygen and transmissivity sensors, a twelve-10l-Niskin bottle rosette and a Seabird Electronics 911 Plus deck unit. The CTD/Rosette unit was coupled on-line to a PC. The raw data set will be post-processed shorebased. Firing sequences for the Niskin bottles were chosen based on the downcast T/S-profiles. Down-cast and up-cast speeds were 0.5 m/s. Close to the sea floor, down-cast speed was reduced to 0.2 m/s. In order to prevent a touchdown on the sea floor. A "pinger" echosounder was used in addition to a bottom sensor to monitor the CTD's approach to the seafloor.

Immediately after retrieval on deck a series of water samples was siphoned off for a suite of geochemical analysis (see below). Water samples for $\delta^{18}O$ and $\delta^{13}C$ analyses were poisoned with $HgCl_2$ to suppress biological activity. Subsequently, these samples where closed airtight with a high-vacuum paste and taped for transport. A set of water samples was sealed airtight in glas bottles for later salinometry to check the calibration of the salinity probe. Stable isotope analysis will be performed on selected water samples post-cruise at the Leibniz Labor for Isotope Research, Kiel University.

Results
The most prominent T-S component in the hydrographic profiles is derived from warm-saline MOW that enters the Gulf of Cadiz at a depth of approximately 280 m. T-S anomalies that are associated with MOW are strongest developed in the northern Gulf of Cadiz where MOW flows along the southern Portuguese margin. Advection of MOW it has resulted in the development of the Faro Drift, a vast sediment body that consists of sediments accumulated and sorted under MOW-related current activities. Acoustic surveys of the Faro Drift show distinct subbottom reflectors that clearly document the current-induced built-up and lateral extension of the Faro Drift (see Figure 57 below) due to the advection of MOW. To trace the evolution of MOW upon its entry in the Gulf of Cadiz and further North, along the western Iberian margin, CTD stations were targeted at the flow path of MOW (Figures 47, 48).

CTD casts from stations in the Gulf of Cadiz, i.e. close to the MOW "point-source" at the Strait of Gibraltar, most distinctly display the vertical T-S-variations into the MOW. At these stations, MOW impinges on the sea floor and is recorded in elevated T-S values in the near-bottom layer (Figure 47) , it is encountered except of cast M39029. At Stations M39017 and M39021, a separation into an Upper MOW (T-S-maxima at 430 and 500 m water depth, respectively) and a Lower MOW was possible (upper boundary at 510 m and 610 m water depth, respectively; Figure 47). Along the MOW flow path, the surface of lower MOW deepens from 500-600 m water depth at Stations M39017 and -021 in the northern Gulf of Cadiz to 1000 m at Station M39029 in the outer Gulf of Cadiz. Maximum MOW temperature at Station M39029 barely

reaches 10°C and remains well below MOW temperatures of > 12°C at stations in the inner and northern Gulf. Likewise, maximum salinities of some 36 at Station M39029 are distinctly lower than those recorded in the immediate MOW flow path where values exceed 36.5 (Stations M39014 and -021; Figure 47). Rapid decreases of T-S values mirror the admixture of Atlantic water masses which results in a continued decrease of the T-S anomaly as one moves out the Gulf of Cadiz and northward along the western Iberian margin (Figure 48).

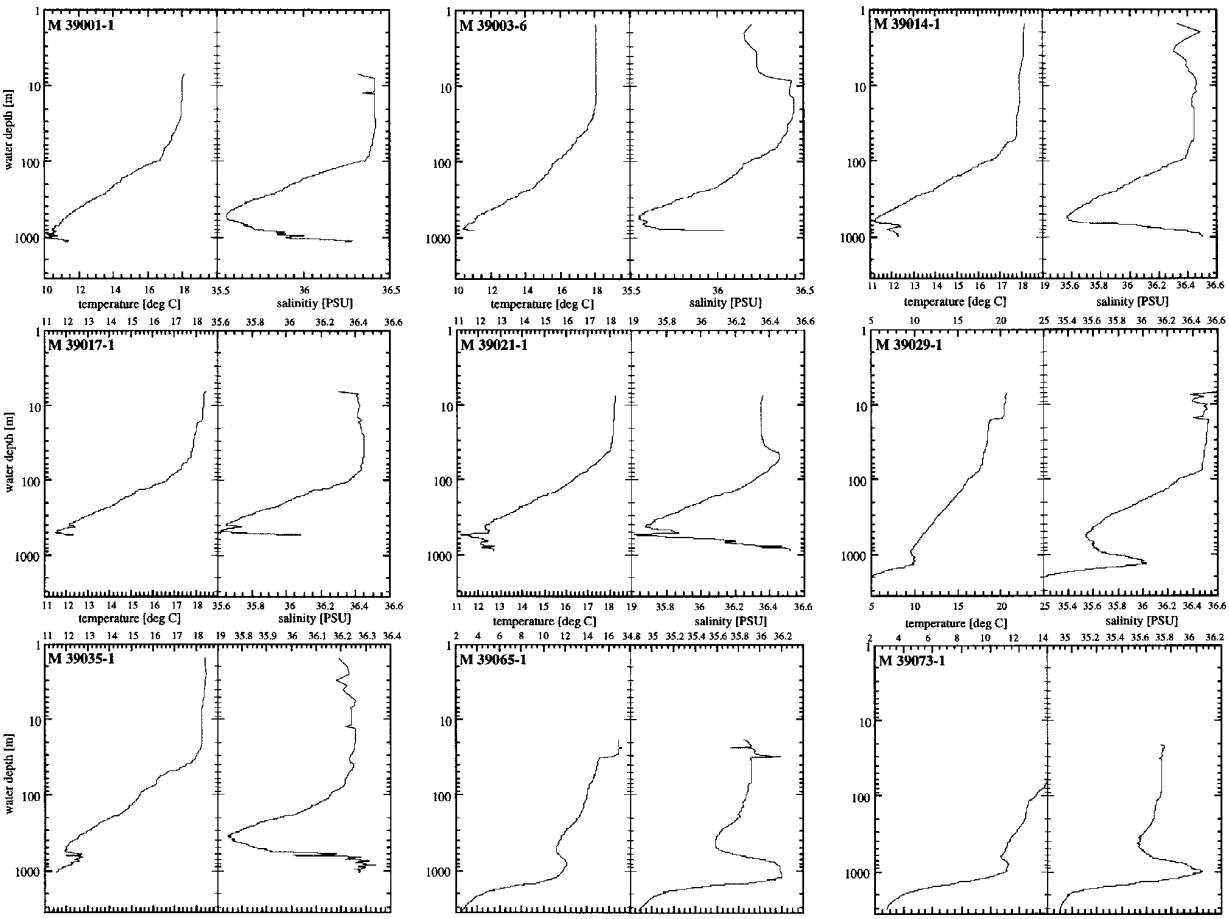

Fig. 47: Water column temperature and salinity profiles from CTD runs in the Gulf of Cadiz (M39001-029) and at the western Iberian margin (M390035-073). CTD stations were targeted at the advection path of MOW. Note logarithmic depth sale that was used to better identify T-S fine structure of the upper water column.

5.4.2 Seawater Sampling for Trace Element and Nutrient Analysis (A. Müller, C. Willamowski)

GoFlo bottles were used to collect water samples for determination of dissolved cadmium. With a bottom weight of 40 kg, 5 to 7 bottles with volumes of 3 x 12 l and 2-4 x 2.5 l were deployed at a time. Down-cast winch speed was 0.5 m/s, up-cast speed was 0.8 m/s. Sampling depths were determined based on the CTD T-S profiles. After recovery, the GoFlo bottles were brought immediately to the laboratory to be emptied under Nitrogen atmosphere. Water samples were

then filtered under clean conditions of a clean bench. 200 ml of each water sample were discarded, 1 l was filtered through a 0.45 µm membrane filter, acidified and stored at + 4°C. Another liter was acidified and stored without previous filtering. Additional samples were taken for onboard phosphate analysis. Because the GoFlo bottles are not equipped with depth sensors, additional water samples were taken from the deepest bottle for salinity analysis. Comparison of the GoFlo salinity values with those from the CTD T-S profiles will serve as a control to monitor GoFlo sampling depths in addition to the wire length readings. Cd analysis will be performed post-cruise at the IfM Kiel.
Water samples for oxygen analysis (double sampling) were taken in 50 ml dark brown glass bottles from each CTD-Niskin bottle immediately after retrieval on deck. After addition of 0.5 ml of alkaline Iodide and 0.5 ml of Manganese (II) chloride, the bottles were vigorously shaken. Prior to analysis, 1 ml of sulfuric acid was carefully added and the bottles were shaken to redissolve precipitated hydroxides. The solution was quantitatively transferred into a beaker with destilled water. Titration was carried out immediately with 0.01 mol/l sodium thiosulphate. Shortly before disappearance of the yellow color, 1 ml of starch solution was added (solution turned blue) and titration finished as soon as the blue color disappeared.

For analysis of phosphorus concentration, 50 ml of seawater from CTD Niskin and GoFlo bottles were transferred to plastic sample containers. Subsamples of either 5 or 10 ml were taken and 0.1 (0.2) ml of two mixed reagents were added (reagent 1: 12.5 g ammonium heptamolybdate tetrahydrate ($(NH_4)_6Mo_7O_{24}$ * 4 H_2O) dissolved in 125 ml distilled water, added to 350 ml of 4.5 mol/l sulphuric acid (while well stirring) - and under mixing added 0.5 g of potassium antimonyl tartrate, ($K(SbO)C_4H_4O_6$) in 20 ml water; reagent 2: 10 g of ascorbic acid in 50 ml of 4.5 mol/l sulfuric acid and 50 ml of distilled water). Samples were transferred into a 5 ml (10 ml) cuvette and absorbency was measured at 880 nm against acidified distilled water as reference. Calibration was carried out with standard solutions of 0 to 2 µmol/l Phosphate. Water column oxygen and phosphorus profiles are shown in Figures 49 and 50. The data will be used for calibration of dissolved carbon isotope and Cd concentrations to regional nutrient inventories.

Water samples for analysis of magnesium, strontium, calcium and CO_3^- concentration were filled into 250 ml PE-bottles. Before use, all bottles were put in a 2% Mucasol-solution for at least one week after which they were rinsed three times with normal water to remove tensids and washed twice and finally filled with Milli-Q water. 1ml of concentrated hydro-chloric acid was added. The bottles were then closed and stored at room temperature for three days, subsequently turned upside-down and again kept at room temperature for three days. Then, the bottles were twice rinsed and filled with Milli-Q water, and finally 1ml of concentrated nitric acid was added to oxidize remaining particles. The containers were then closed and remained at room temperature for three days. This step was repeated after turning the bottles upside-down. Finally, the bottles were rinsed twice with, and then filled with Milli-Q water. For conservation, 5 drops of concentrated nitric acid were added. The bottles were closed, sealed with parafilm, wrapped in foil, and stored at 4°C. The first step of the pre-sampling treatment of the duranglas bottles (250 ml/350 ml) that were used to sample for CO_3^- analysis consisted of a one day bath in 61°C hot solution of Mucasol (3%) to remove fatty compounds. Then, these bottles were rinsed once with destilled water and three times with Milli-Q water in order to remove tensids. Finally, they were dried at 62°C and wrapped in foil.

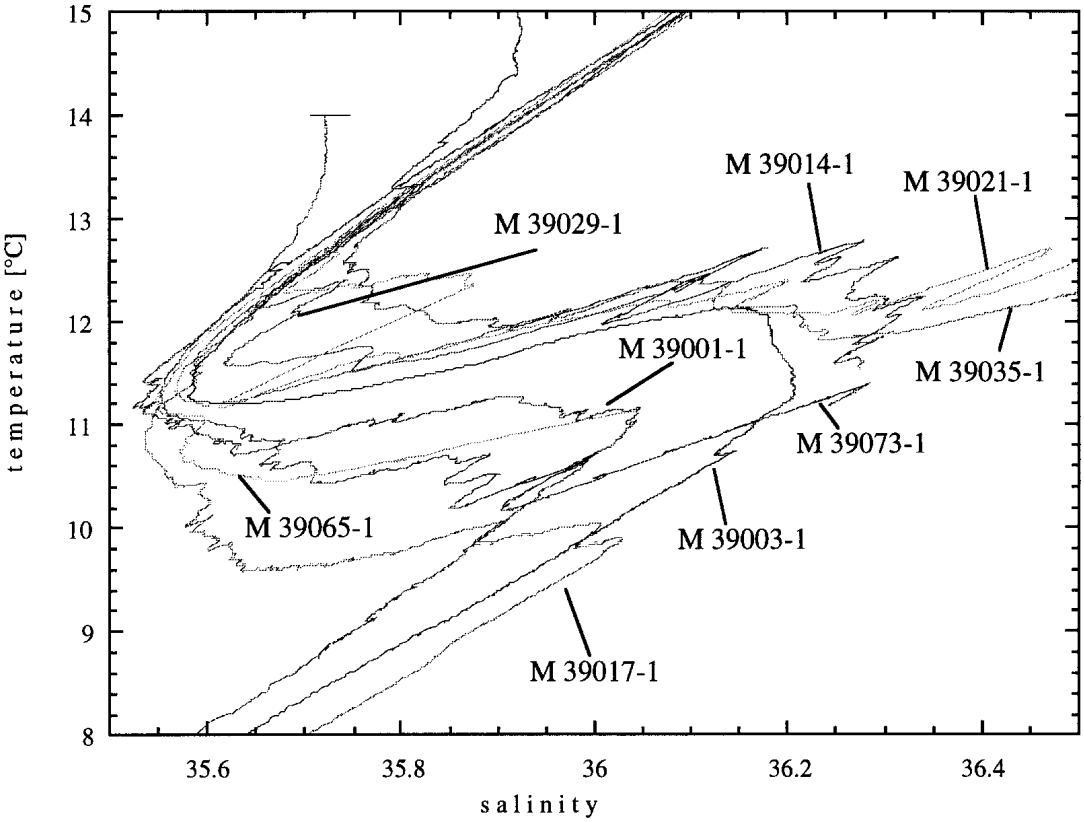

Fig. 48: T-S diagramm showing the hydrographic anomaly that is associated with the advection of warm and saline MOW. Strongest T-S anomalies are recorded at stations close to the immediate flow path of MOW in the northern Gulf of Cadiz (Stations M39001, -014, -017, -021). Decreased T-S values are observed in the outer Gulf of Cadiz (M39029) and at the northern section of the western Iberian margin (M39065, -073) documenting the continued admixture of Atlantic waters.

Immediately after retrieval of the CTD/rosette water sampler (Multicorer) on deck, 250-350 ml of seawater for CO_3^- analysis were siphoned off the Niskin-bottles to prevent CO_2-exchange with the atmosphere. The head space of the filled sample bottles was kept below 2%. All samples were poisoned with saturated mercury-II-chloride-solution (250 ml bottles with 50µl saturated mercury-II-chloride-solution and 350 ml bottles with 75µl saturated mercury-II-chloride-solution). The bottles were immediately closed with a Duranglas cap lubricated with Apizon-L, and subsequently sealed airtight. In a second sampling run, 250 ml of seawater (for Mg, Sr-analysis) were taken from the CTD-bottles and Multicorer tubes (the PE-bottles were emptied 1-3 h before). Prior to sampling, each bottle was washed three times with sea water. For conservation, 5 drops of hydrochloric acid were added. The bottles were then closed, sealed with parafilm, wrapped in foil, and stored at 4°C. Trace metal analysis will be performed shorebased in cooperation with the IfM Kiel.

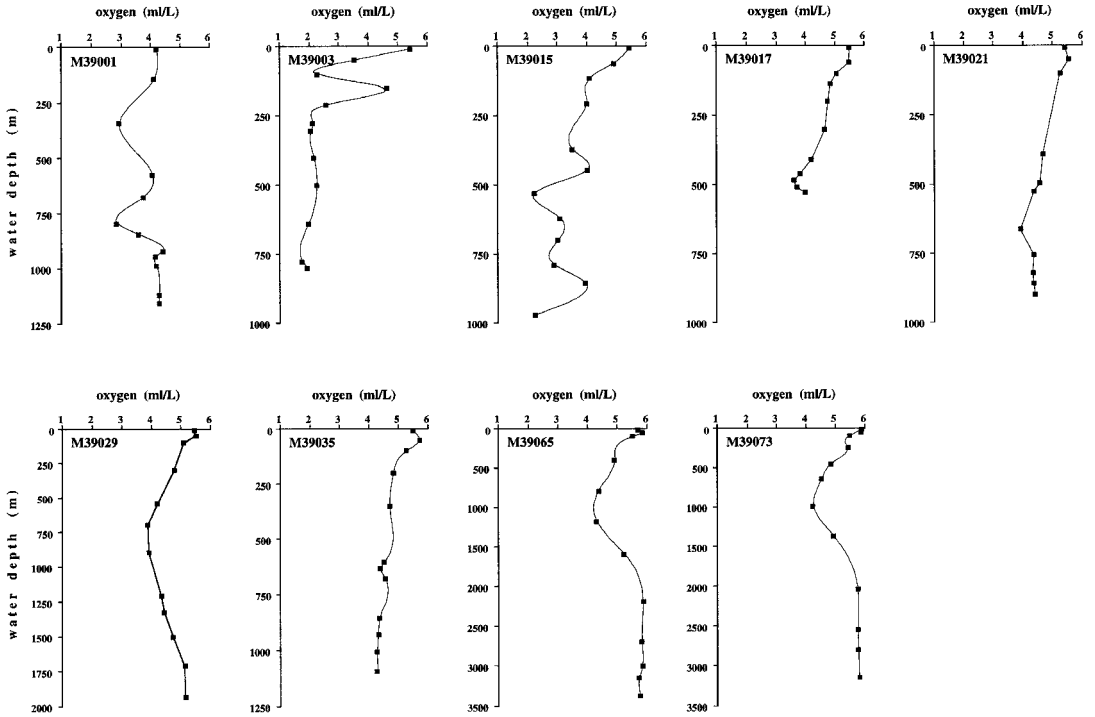

Fig. 49: Water column titration oxygen profiles from Niskin bottle water samples in the Gulf of Cadiz (M39001-029) and at the western Iberian margin (M39035-073). See Figure 2 for hydrocast positions.

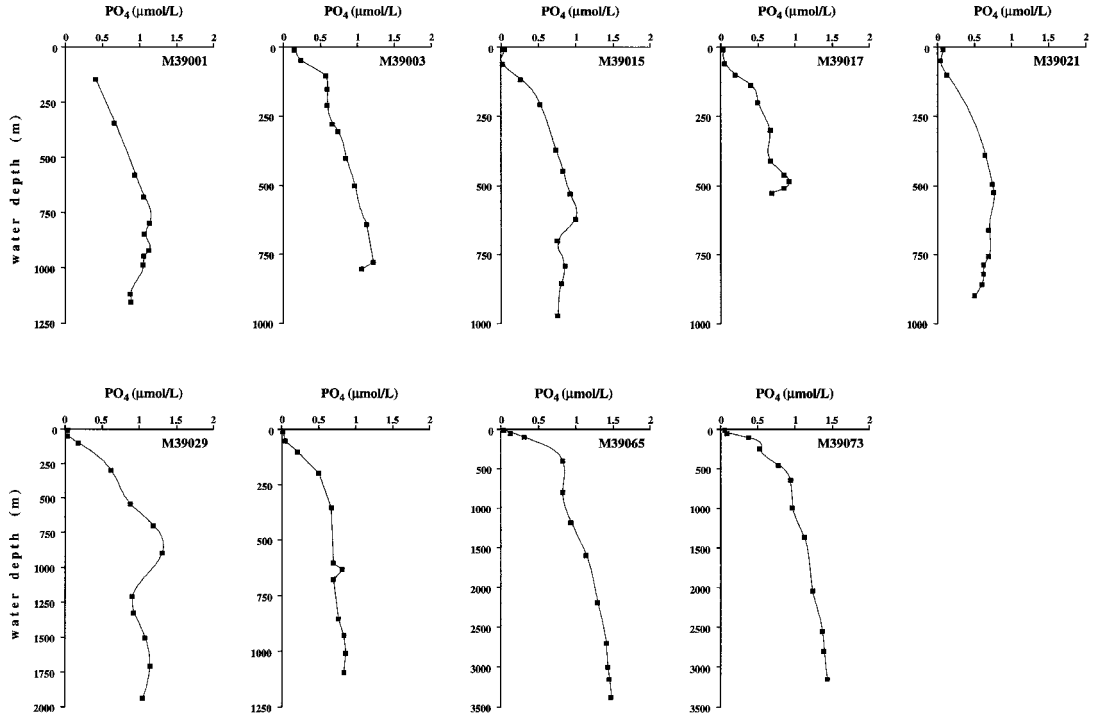

Fig. 50: Water column phosphate profiles from Niskin bottle water samples in the Gulf of Cadiz (M39001-029) and at the western Iberian margin (M39035-073). See figure 2 for hydrocast positions.

5.4.3 Shipboard Sediment Sampling and Core Flow (G. Bozzano, C. Didie, M. Huels, S. Jung, L. Lembke, N. Loncaric, P. Schäfer, J. Schönfeld)

During M39/1 a gravity -, box-, and Multicorer as well as a grabber and a dredge were deployed for sediment sampling. Subsampling according to the detailed sampling schemes (Figures 51, 52; Table 11) was restricted to sampling of box cores, slicing of multicorer tubes, washing of grab samples and dredged material. Sampling of sediment cores was mostly postponed to a post-cruise sampling party to facilitate standard laboratory procedures and precise determination of physical properties. After retrieval of the sediment cores on deck, they were cut into 1 m sections and subsequently routinely run through the core logger. Only few sediment cores were opened for visual inspection of sediment composition and core quality. These cores were routinely cut into working and archive halves. Macroscopic core description, color scanning and core photographs were done on archive halves while sediment samples were taken from working halves.

Table 11: Shipboard Sample Distribution Scheme

Investigator	Device	Sample Interval	Volume
B. Bader/P. Schäfer	GKG[1], BG[2], Dredge[3]	surface[1], whole sample[2,3]	100 cc[1], macrofauna[1]
G. Bozzano	SL[1,2], GKG[1]	5 cm[1], 1 m[2]	10 cc[1], 4 cc[2]
S. Jung/R. Zahn	GKG[1], SL[2]	0, 2, then 5 cm[1], 10 cm[2]	10 cc
A. Kohly/C. Didi	MUC[1], GKG[2],	1 core[1], top of archive core[2]	100 cc[2]
N. Loncaric	MUC[1], (GKG[2]), SL[3]	1 core[1], 10 (5) cm[2,3]	1-3 cc and 20 cc
A. Müller	MUC[1], GKG[2]	1 core[1], surface[2,]	100 cc[2],
P. Schäfer	MUC[1] GKG[2], SL[3]	1 core[1], archive core[2], entire section[2,3] (x-ray), surface[2]	x-ray slabs[2,3], 100 cc[2]
J. Schönfeld	MUC[1], GKG[2], SL[3]	1 core[1], surface[2], 5 cm[3]	3 x 88 cc[2], to be shared with Anja Müller[3]
C. Willamowski	MUC	1 cm	2 cores
U. Pflaumann (onshore)	GKG	0, 2, then 5 cm	10 cc

MUC: multicorer, GKG: box corer, BG: Van Veen grab, SL: gravity corer

The color scanning system consisted of a hand held Minolta photo-spectrometer and a transformer. The photo-spectrometer was coupled on-line to a Macintosh Powerbook 170, on which the ODP-software package “Spectrolog” was run for data management. During the color scanning, the sediment sections were covered by ceran wrap to prevent sediment smearing onto the measuring unit. Sediment cores were routinely scanned at 2 cm intervals.

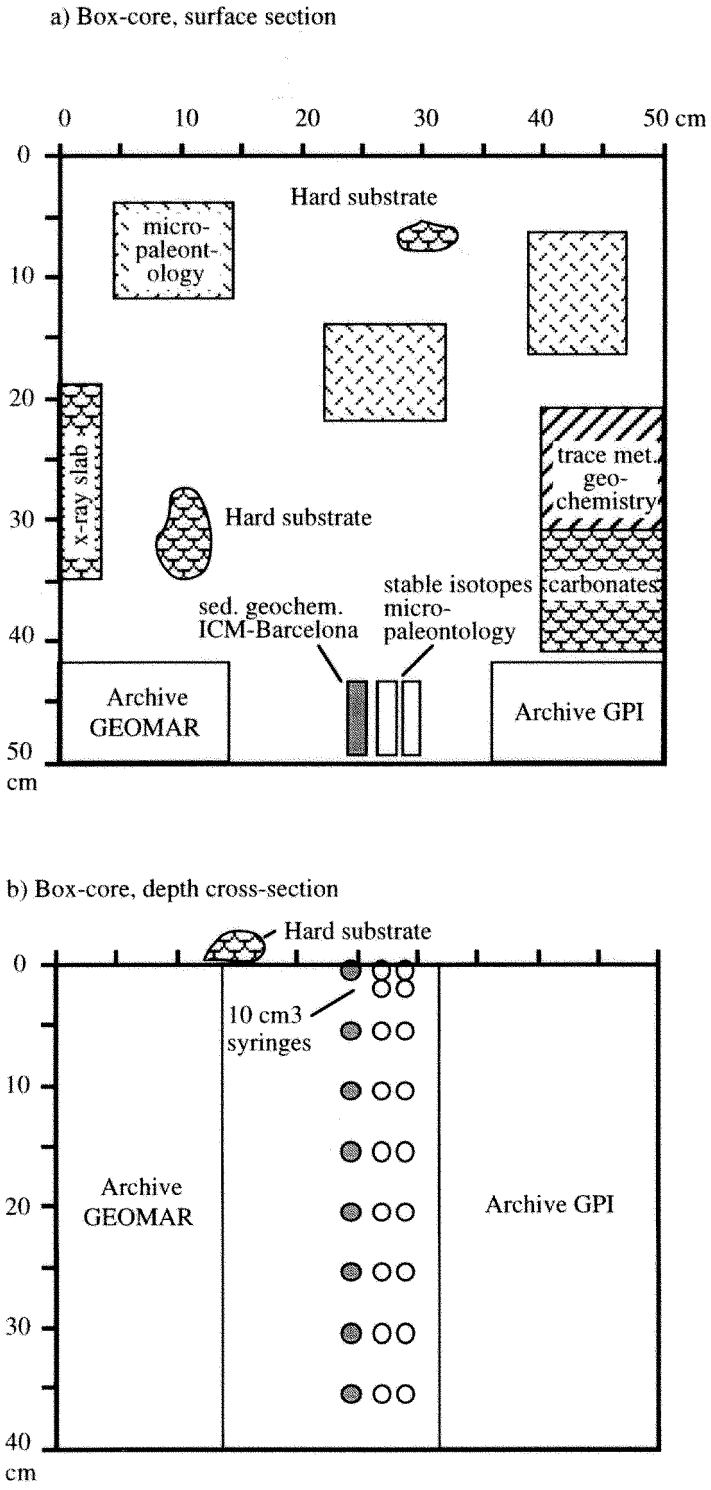

Fig. 51: M39/1 sampling scheme for Giant Box Core (GKG) sampling.

5.4.4 Plankton Hauls (A. Kohly)

Methods

To study the transfer of living plankton assemblages (and its change) into the sediment, plankton net hauls, filtered water samples from the CTD, and sediment samples were taken. In total, 32

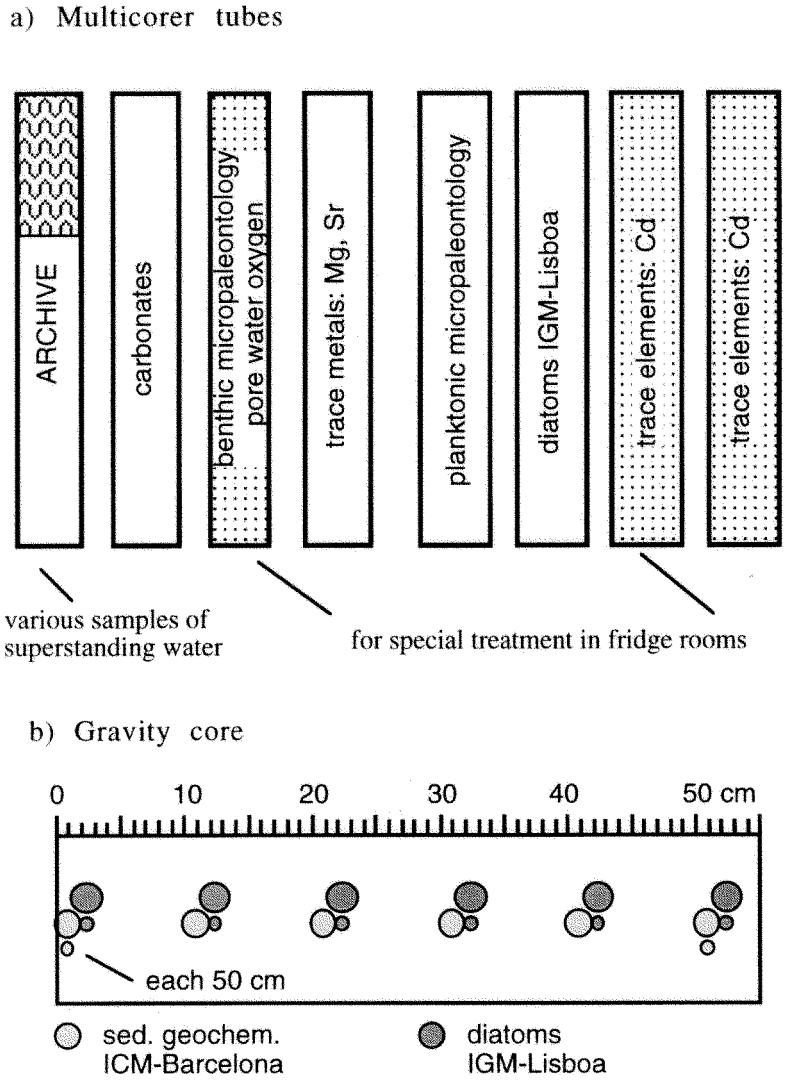

Fig. 52: M39/1 sampling schemes for (a) multicorer tubes, (b) gravity cores. Detailed sampling of gravity cores will be done post-cruise in collaboration with shore-based scientific partners.

plankton hauls (mesh width 20 µm) from the uppermost 10-12 m were taken. All samples were treated with Formalin to stop biological activity. After settling, 3-4 drops of the concentrated plankton material were placed on a cover slip for on board microscopic analysis. The seston of mostly two liters of CTD/rosette water samples was (vacuum) pumped through a cellulose membrane filter with a pore width of 45 µm (diameter of 5 cm) (list 7.1.2). After drying, the filters were placed in plastic petri dishes, sealed in plastic bags and kept dry by using silica gel. This material will be used to investigate the vertical distribution of coccolithophors and diatoms and to compare it with the species distribution in the underlying surface sediments and sediment cores. Detailed scanning electron microscope (SEM) analyses on the plankton samples will be carried out post-cruise.

Results: Phytoplankton and Zooplankton

Diatoms were the most abundant plankton group in most of the samples. Mainly fragile species such as *Proboscia alata, Bacteriastrum hyalinum, B. delicatulum, Guinardia flaccida,*

Rhizosolenia fragilissima, R. delicatula and several species of the genus *Chaetoceros* were found. At one station (M39073), coincidentally a bloom of *Proboscia alata* was sampled . A list of identified phyto- and zooplankton species or groups is given in list 7.1.3. Dinoflagellates were the second most abundant plankton group; at Stations M39001, M39002, M39003, M39017, M39058 they even dominate the plankton community. Species of the genera *Ceratium, Dinophysis, Peridinium,* and *Prorocentrum* frequently occurred, whereas genera *Ceratocorys, Oxytoxum, Gonyaulax* and *Diplopeltopsis* were less abundant. Specimens of *Actiniscus pentasterias* solely occurred in samples M39006 and M39025 (list 7.1.3). Coccolithophorids were merely sampled at single stations, and never reached high concentrations. These lower than expected concentrations are probably due to the inappropriately coarse mesh width for sampling the small sized coccoliths. Furthermore, silicoflagellates (*Distephanus speculum* and/ or *Dictyocha fibula*) occurred in almost 50 % of the samples.

Tintinnids were the most abundant zooplankton organisms in the net hauls. Several genera were observed such as *Amphorides, Rhabdonella, Parafavella, Steenstrupiella, Dictyocystis, Tintinnus, Dadayiella* and some others with uncertain identification. Radiolarians occurred in small amounts and initial stages of their skeletons were frequent at a few stations. Both spinous and non-spinous species of planktic foraminifera were present in the net hauls.
Macro-zooplankton larvae of different organisms such as copepods and polychaets were present in most of the samples, occasionally reaching significant abundances.

In general terms, the highly diverse diatom assemblage is typical for warm water regions. The lack of spore specimen in the vegetative cells of *Chaetoceros* species indicates, that the bloom cycle had not been completed. *Chaetoceros dadayii* and *C. tetrastichon*, warm water (mediterranean type) diatoms were observed with the parasitic tintinnid (*Tintinnus inquilinus*). Areas with low diatom content (outer Gulf of Cadiz), are dominated by dinoflagellate species. This group shows a dominance of species of *Ceratium, Peridinium,* and *Gonyaulax*. Possibly, the diatom bloom had finished at these stations or else the surface water was too oligotrophic for high diatom abundances.

5.4.5 Porewater Oxygen Profiling: Reference for Benthic Foraminiferal Assemblage Studies (J. Schönfeld)

Methods
The profiling instruments were mounted in a shipboard temperature-constant laboratory ("Gravimeter-Raum"). A Diamond General 768-20R needle oxygen electrode was fixed in an aluminium tube which was centered in the multicorer tube attached to the frame (Figure 53). The multicorer tube was pushed upwards with a standard laboratory lifting platform, while the electrode remained in a fixed position so that the needle was driven into the sediment. The penetration depth is displayed on a scale at the platform. The electrode current was measured with a conventional picoamperemeter. Electrode specifications and measuring procedures are described by DIAMOND GENERAL (1997).

Ambient laboratory temperature was set to the expected bottom-water temperature at least twelve hours before the measurements. The room temperature was kept constant during the measurements with variations of ±0.25°C. The electrode was stored in deionized water during transit times and was submersed in seawater at least 4 hours before the measurements for stabilization. Calibration of the electrode was done immediately before the measurements by relating the current measurements to oxygen concentrations of two water samples which were subsequently analyzed by using a standard Winkler method (GRASHOFF, 1983). First, we determined the dissolved oxygen content of the superstanding water of the multicorer, i.e. the bottom water. A second calibration point at low oxygen values was obtained by analyzing a seawater sample through which nitrogen was bubbled for at least 30 minutes.

Immediately after retrieval of the multicorer on deck, one tube was sealed with two rubber plugs and brought to the temperature-constant laboratory. The upper lid of a second tube was opened and the overstanding seawater was transferred into two Winkler bottles for bottom-water oxygen determination. Prior to porewater oxygen analysis with the needle probe, overstanding seawater was carefully siphoned off down to a level of 1 to 3 cm above the sediment surface. The tube was then set on the lifting platform, fixed to the frame and the tip of the electrode was moved down to a level of one millimeter above the visual upper boundary of the bottom nepheloid layer, and was fixed there. The measurement at this point was related to the oxygen concentration of the overstanding water. Oxygen readings were allowed to stabilize for 12 to 30 minutes. When the readings remained constant for more than five minutes, the data were recorded . The lifting platform was then moved upwards a few millimeters for the following measurement. The values were recorded down to either that level below the sediment surface at which the electrode current remains constant or the maximum length of the needle and holder, i.e. 80 mm.

After the measurements, the needle probe was cleaned and submerged in deionized water. The sediment was pushed out of the core tube and was cut into 5 or 10 mm thick slices which were conserved in a Rose Bengal Methanol solution.

Results: Porewater Oxygen Profiles in Selected Surface Sediment Samples

Pore-water oxygen profiles were measured at four multicorer stations, three from the Gulf of Cadiz (M39002-3, M39003-2, and M39029-6 at 1209, 800, and 1918 m water depth respectively) and one station off Cape Sines (M39035-3 at 1082 m water depth). The depth distribution of dissolved oxygen in the pore waters display a characteristic exponential mode as expected from theoretical models (BERNER, 1980; GOLOWAY and BENDER, 1982). The shape of the curves is very similar at the shallower sites whereas the deep-water site displays a much lower gradient (Figure 54). The redox boundary was recorded at depths between 3.9 and 7.1 cm below the sediment surface at the shallower sites and it was not encountered at the deep-water site from the Gulf of Cadiz indicating that oxygen consumption is low here. Relations to C_{org} contents and sedimentation rates have to be tested and will be a subject of post-cruise studies. The boundaries between low oxic, suboxic, and dysoxic pore waters are documented at different sediment depths in each core thus offering a good opportunity for a core-to-core comparison of the depth distribution of deep infaunal species as a function of oxygenation levels at different depths in the sediment.

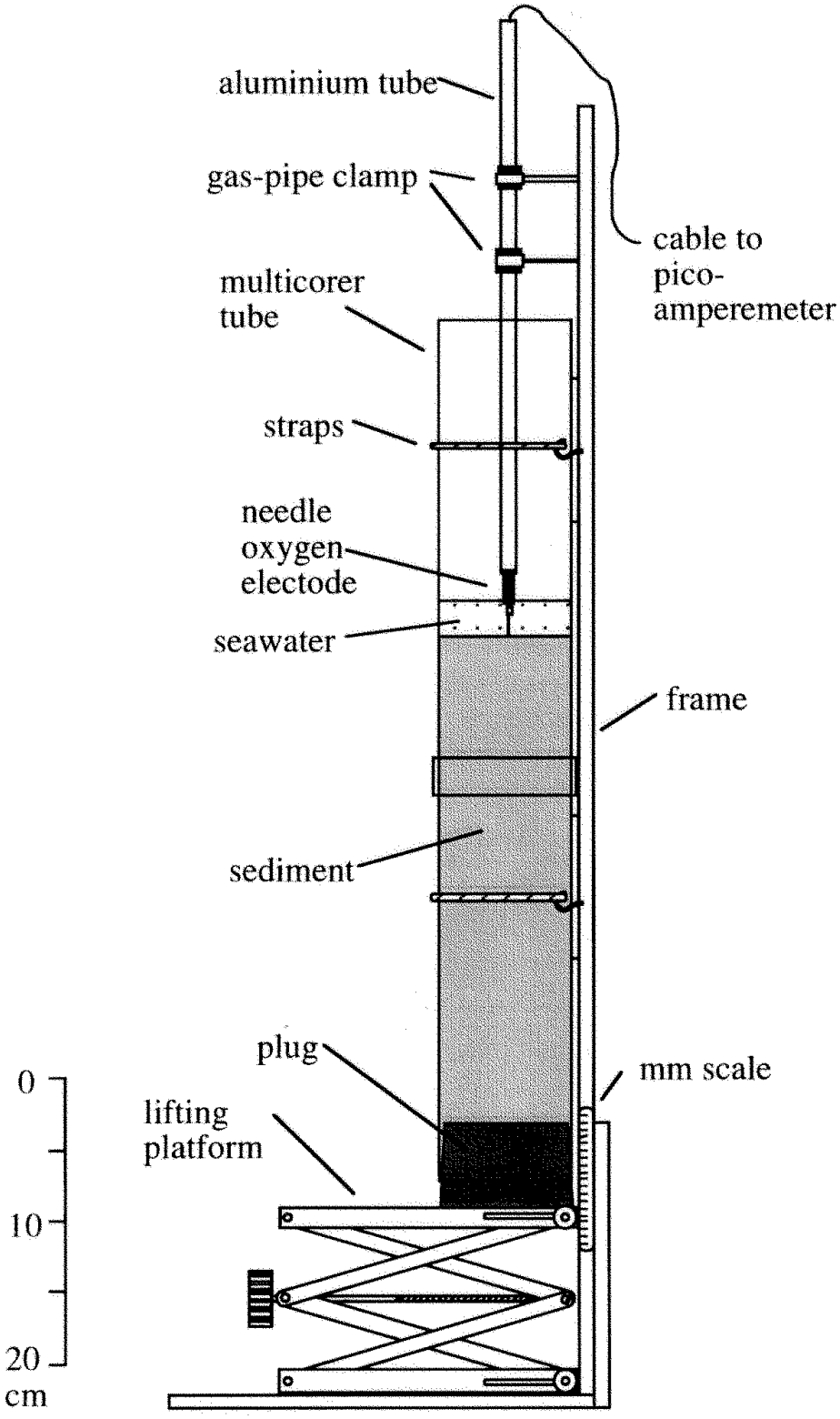

Fig. 53: Laboratory rack with oxygen needle-probe for porewater oxygen measurements. Ambient temperature in the laboratory was held constant at 8°-14°C, depending on locval bottom water temperature from where the core was retrieved.

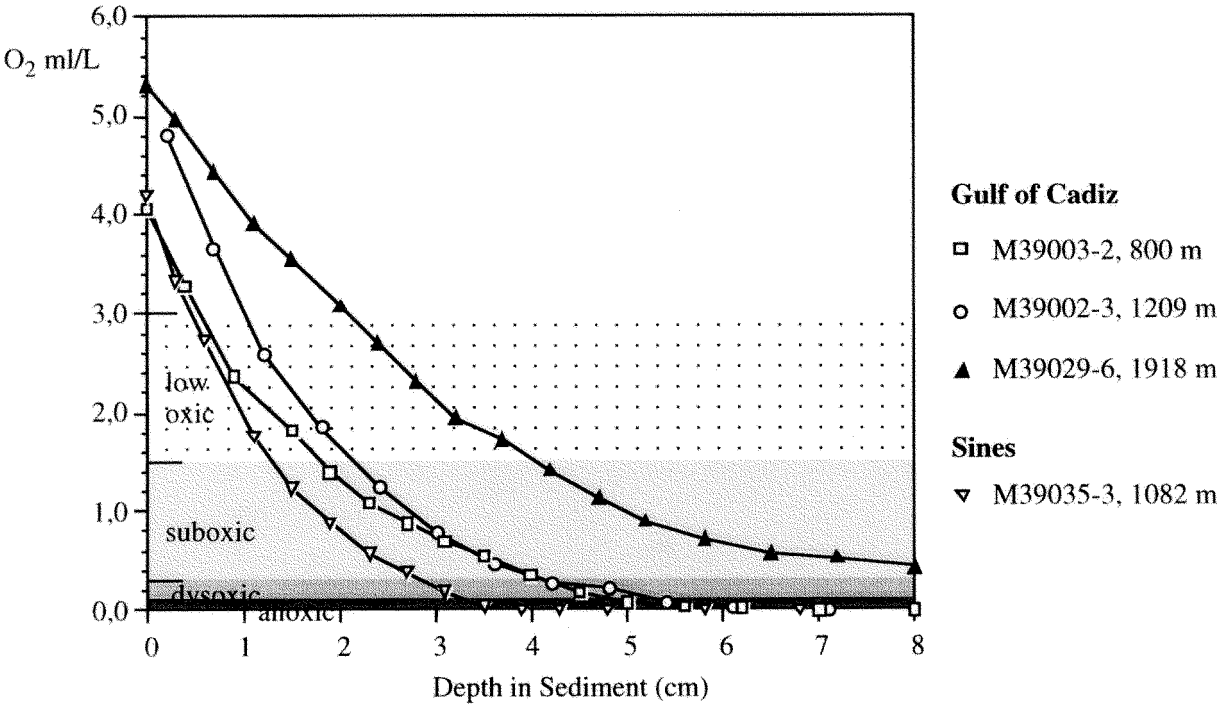

Fig. 54: Porewater oxygen profiles at four stations in the Gulf of Cadiz and off Cape Sines. Differential penetration depths of oxygen likely are a function of sedimentation rare and bottom water oxygen concentration. The data will serve as estimators for environmental control on the depth distribution of infaunal benthic foraminifera.

5.4.6 Trace Fossil Recording and Grab Sampling (P. Schäfer, B. Bader)

a) Instrumentation and Sample Conservation

Sediment samples were taken from within and outside the drift sediments in the Gulf of Cadiz as well as from three primary areas along the western Iberian continental margin at water depths of 110 to 2170 m i.e., across the MOW flow path. At least one radiograph was taken from each giant box core. Following a standard technique developed at the GPI Kiel, a thin slab was taken from each box core using a plexiglas cover of 27 to 15 cm size and 1 cm thickness, then put into plastic bags, evacuated, sealed, and stored at 4°C. Radiograph sampling of gravity cores will be done onshore.

Additional sediment samples taken with Van Veen grab and giant box core were archived in plastic bags and liners and were stored in the shipboard reefer. Surplus sediment was washed on deck through a sieve to retain the coarse fraction >1mm. This was especially important, were the carbonate content was low due to strong terrigenous input (siliciclastic sediments of the Faro drift; glauconitic quartz sand apron between 200 and 500 m water depth along the Western Iberian continental margin). Living organisms were stored in 70% alcohol or 10 % formaline buffered with sea water.

b) Trace Fossil Assemblages

In general, all sediments show strong bioturbation that covers nearly the complete sediment column. *Preservation/intensity* of bioturbation, however, is poorest in the upper 5 cm of the sediment column ("Homogenous top layer" after WETZEL, 1981) and in sediments from shallow sites. A pronounced trace tiering was found in sediments from deep water sites. Both vertically and horizontally arranged feeding traces do occur. Burrows of crustaceans were observed in giant box cores as conical mounds of 5cm height; they were commonly found at shallow sites in the Gulf of Cadiz. They occur as vertical burrows with uneven burrow lining in radiographs. A preliminary description of trace fossils is given in Table 12.

At first inspection, radiographs taken from box core material revealed trace taxa of *Scolicia, Planolites, Teichichnus, Chondrites, Helminthopsis* and *Trichichnus.* On shore radiographs from gravity cores taken during METEOR cruise M39/1 (and additional material will be collected

Table 12. Trace Fossil Occurrence in the Gulf of Cadiz and at the Western Iberian Margin Sites

Sample	water depth	Onboard sediment/trace description	
M39002-2A	-1209m	*Zoophycos, Scolicia, Chondrites* trace tiering	
M39002-2B	-1209m	poor trace record	trace tiering
M39003-1A	-801m	*Planolites,* trace tiering	
M39003-1B	-801m	*Teichichnus, Planolites*	*Zoophycos,* trace tiering
M39004-1	-966m	*Chondrites, ?Helminthopsis*	*Zoophycos,* ?Planolites
M39005-3	-118m	poor trace record	
M39006-1	-214m	crab burrows	
M39009-1	-681m	*Chondrites, ? Planolites*	poor trace tiering
M39010-1	-878m	Sand layer overlying silt layer	poor trace record
M39016-1	-581m	poor trace record	
M39017-5A	-533m	poor trace record	
M39017-5B	-533m	poor trace record	
M39018-1	-496m	poor trace record	
M39019-2	-730m	*?Teichichnus, ?Planolites*	poor trace tiering
M39020-1	-726m	trace tiering	
M39021-5	-901m	Sand layer overlying silt layer	poor trace record
M39022-1	-668m	trace tiering	
M23023-2	-730m	*?Planolites, ?Trichichnus*	trace tiering
M39029-3	-1917m	*Zoophycos, Planolites*	trace tiering
M39036-1	-1747m	*Trichichnus*	trace tiering
M39037-3	-2532m	?Helminthopsis	
M39058-1	-1975m	*Helminthopsis, Lophoctenium*	*Planolites*
*M*39059-2	-1605m	*Zoophycos*	
*M*39061-1	-544m	poor trace record	trace tiering
M39070-1	-1220m	sand layer overlying silt layer	poor trace record
M39072-1A	-2170m	*Scolicia, Zoophycos, Planolites*	trace tiering
M39072-1B	-2170m	*Scolicia, Zoophycos*	trace tiering

during METEOR cruise M40/1 into the Mediterranean Sea) will be studied in detail. These analysis include a visual description of bioturbation phenomena in sediment cores, the analysis of trace morphology and of trace associations from radiographs, and finally computer tomographic scans and image processing of traces in order to better illuminate their three dimensional structure. Stratigraphic and sedimentary analysis will be done post-cruise in conjunction with stable isotope analyses.

c) Sediment Composition

A depth transect was sampled in the Gulf of Cadiz at water depths between 100 and 800 m along which Van Veen grab, sediment dredge, giant box corer and gravity corer were deployed. The transect was chosen so as to span the depth range of MOW and water masses immediately above and below. The Faro Drift was an important target area in the Gulf of Cadiz (Figure 2).

At the southern Portuguese margin, a depth transect from 50 to 500 m water depth was sampled with the Van Veen grab and the sediment dredge. Further samples were taken with a Van Veen grab and dredge from the isolated pinnacles of the Principes de Avis as well as from the Tejo Plateau off Cap Finisterre, grab and dredge samples were taken from 50 to 80 m water depth. Off NW Galicia, a spur of the continental shelf elevating up to 400 m water depth was sampled with a Van Veen grab. Further sediment samples were taken with a giant box corer from deeper water locations.

Sediment dredge sampling revealed pebbles and solid rock fragments, lithified coral framework and some living macroorganisms such as corals, bryozoans, and echinoids. A large amount of ship slag occurred in sediments below the major ship route in the Gulf of Cadiz and around Cabo de São Vicente. It showed intensive overgrowth by epibenthic organisms such as hydrozoans, sponges, bryozoans, serpulids, polychaetes, bivalves, and sessile foraminifers. Most of the material was dried, only few slag pieces were stored in 70% alcohol.

Van Veen grab and giant box core samples were taken along a profile in the Gulf of Cadiz between 36°03,0N/007°13,8W and 36°31,9N/006°44,0W at water depths between 110 to 850 m. Parasound profiles displayed a gentle topography and sediment accumulation is indicated by several parallel reflectors. Sediments typically consist of bioturbated siltic clay to clayish silt, partly with bivalve coquinas. Surface sediments typically consist of fine- to medium grained sand with abundant biogenic fragments (echinoid spines, gastropods, bivalves, corals and bryozoans). High abundances of endobenthic species indicates a high content of fine sediment fraction (i.e. compared to the carbonaceous lag deposits in high boreal to subpolar shelf settings; SCHÄFER et al., 1996; HENRICH et al., 1997).

The deepest sampling locations (M39013-1; M39014-1,2) are characterized by a rough topography on the Parasound/Hydrosweep profiles. The sediment dredge recovered solid rocks and pebbles of red, fossiliferous sandstone colonized by a diverse epifauna (hydrozoans, bryozoans, ascidians, serpulids, actinians). Coral fragments, sea-urchins (*Cidaris cidaris*) and gastropods also occurred.

Typical deep water coral reefs were not found but the considerable abundance of coral fragments in sample M39014-2 implies the nearby presence of reef-like coral structures. The coral fragments show strong alteration (corrosion, bioerosion, epigrowth) and cementation, that either suggest a fossil age of the fragments or unusually early cementation. The lack of fine grained sediment and the abundance of sessile epibenthic suspension feeders are indicative of strong bottom currents (MOW).

The Faro drift consists of sandy, silty, and muddy contourites. The clayish silt to fine sand of the contains mainly endobenthic bivalves, associated with large solitary corals (*Flabellum* sp.) and terebratulid brachiopods. Due to increasing sediment coarseness at sites closer to the coast, the robust Van Veen grab was used at several near-shore sites. Except for a narrow erosion belt, which is indicated by slightly greater water depth and coarser sediments, clayish silt occurred up to shallowest depths of 103 m.

Sediments on the flanks of the Découvreur seamounts (M39030 to M39034) consist of silty fine to coarse sands that are enriched in pteropods, sponge spicules, and benthic and planktonic foraminifers. The tops of these seamounts are covered by blankets of coarse sand and fine gravel with high carbonate contents. This sediment includes a rich epibenthic fauna dominated by bryozoans, bivalves, and gastropods. Sediment distribution and facies types of the Découvreur seamounts correspond to that on the Principes de Avis. However, samples from the latter revealed siliceous sponges and ophiuroids.

A depth transect off Sadao (M39047 - M39054) covers the upper shelf slope between 500 and 100 m water depth and retrieved glauconitic medium to coarse sands with a high contents of small bivalves, gastropods, echinoid spines, benthic foraminifers, and skeletal debris. Sediments at depths shallower than 100 m are characterized by coarse sands with variable carbonate contents, and by well rounded pebbles 10-15 cm in diameter that were intensively encrusted by bryozoans, coralline red algae, and the foraminifer *Minicea minima*. An apron of glauconitic medium to coarse sand covering the outer shelf and uppermost slope that is found along the entire western Iberian continental margin was tracked up to the northernmost M39/1 sampling sites off Galicia.

The Tejo Plateau presumably is the most extended shelf area on the western Iberian margin where biogenic carbonate production and accumulation occurs between 50 and 200 m water depth. Coarse sand and fine gravel with a high carbonate content was found on the Tejo Plateau in water depths of 160 m. The coarse fraction >2 mm is composed of bivalves, gastropods, erect bryozoans, skeletal fragments of cirripedians (*Verruca stroemia*), and serpulids. The fraction 1-2 mm is dominated by branchy bryozoans, bivalve debris, and benthic foraminifers. Interestingly, at Tejo Plateau the epifauna dominates the endofauna in contrast to the Gulf of Cadiz and the glauconite sand apron along the Portuguese coast. The distribution of carbonate rich sediments apparently is linked to the delivery of terrigenous material. Off Tejo Plateau, on a topographically isolated submarine mound (132 m below the sea surface) angular pebbles and solid rocks up to 50 cm in diameter were collected that were intensively overgrown by *Miniacea minima*, a diverse encrusting bryozoan fauna, and serpulids.

Off Cabo Finisterre, sites between 500 and 200 m water depth revealed a glauconitic medium to coarse sand apron. Solid rocks in water depths of 50 to 70 m were colonized by large bryozoans and corals. Solid rocks seem to be the preferred habitat for the epibenthic fauna, whereas endofaunal elements are present in glauconitic sand aprons and drift sediments.

Along the northern margin of Galicia, the shelf is bordered by a fracture zone forming a very steep topographic relief cascading into the deep Gulf of Biscaya. Glauconitic sands, poor in carbonate were found up to the northernmost position. Framed by steep walls, solid rock is exposed in 500 m water depth. Pebbles and rock boulders collected with a dredge show intensive overgrowth by sponges, bryozoans, serpulids, and benthic foraminifers. Post-cruise studies include sediment component analysis including carbonate and organic carbon contents, radiocarbon datings of carbonate skeletons, (paleo-) ecological analysis of dominant organisms, taphonomic analysis of carbonate skeletons (bioerosion, mechanical destruction, transport processes), characterization of areas of carbonate production and accumulation, and carbonate budget, terrigenous component analysis (reconstruction of sediment origin and transport patterns), and analysis of microorganisms: benthic and planktonic foraminifers, diatoms, and ostracods.

5.4.7 Geochemistry and Mineralogy (G. Bozzano, I. Cacho)

From all opened cores samples were taken shipboard for various sedimentological and geochemical analysis. Surface samples will be used to study clay mineralogy and some cores will be selected for studying the complete mineralogical record. Additionally, three gravity cores (M39002-6, M39004-5, M39029-7) were wide spaced sampled (every 50 cm) onboard for a prospective molecular biomarker study. A total of 32 samples was collected by a 2.5 ml syringe (1 cm), stored in glass vials and immediately frozen. These samples will be processed post-cruise to determine the quality of the samples for molecular biomarker analysis. According to these results one core will be selected for a high resolution study (every 2 cm). The analysis will focus on a series of molecular biomarkers originated by marine and terrestrial organisms: C29 n-alkane, C26 n-alkan-1-ol, phytol and long chain di and tri-insaturated alkenones (37 and 38 carbons). These compounds are present in most marine sediments and, after a lipid extraction, they can be clearly identified and quantified by gas-chromatography. Their abundance records serve as proxies either for marine paleoproductivity (Phytol and long chain alkenones) or for terrestrial input (C29 n-alkane and C26 n-alkan-1-ol). Furthermore, these compounds enable a reconstruction of the past sea surface temperature (Uk 37 unsaturation index).

5.4.8 High-Resolution Acoustic Mapping and Core Logging: Paleoceanographic Application (K. Heilemann, F.-J. Hollender, T. Karp)

a) Instrumentation

Parasound and Hydrosweep profiling during M39/1 concentrated on sediment drifts in the northern part of the Gulf of Cadiz and were carried out as part of the STEAM MAST Project. R/V METEOR's Parasound echo-sounder applies two simultaneous primary frequencies (a fixed frequency of 18 kHz and a variable frequency of 18 to 23.5 kHz). Due to a Parametric Effect in water, a secondary frequency is produced (2.5 to 5.5 kHz). In ocean sediments a penetration of up to 100 m can be reached. Onboard, paper plots were used for prospective studies, digital data were stored on magnetic tape for post-cruise processing. The Hydrosweep system, a multibeam echo sounder system operates at a frequency of 50 kHz. The combined use of Parasound and Hydrosweep allows a three-dimensional imaging of superficial acoustic units.

Sediment cores were logged using a GEOTEK Multi Sensor Core Logger (MSCL; P. SCHULTHEISS, GEOTEK, Surrey, UK) that provides continuous, high resolution and non-destructive measurements of physical properties that are used for stratigraphic correlation and lithologic interpretation. The MSCL used during M39/1 consisted of a p-wave logger (PWL; determination of compressional wave velocity), a gamma ray source (^{137}Cs and detector; estimation of sediment density), and a Bartington magnetic susceptibility meter. The system is fully computer-driven. Whole-round core sections were placed on a core boat and transported by a stepper motor through the tracking system for a high resolution measurement (2 cm) of physical properties. Data files are stored in ASCII format.

The p-wave-logger consists of two transducers, which send and receive a 500 kHz ultra-sound signal through the core at a rate of 1 kHz. The travel time of the signal and the diameter of the sediment core are used to calculate p-wave velocity in the sediment. The true diameter of the core liner is monitored for each measurement by an electronic caliper. A detailed discussion of MSCL application is given in SCHULTHEISS and MIENERT (1988) and SCHULTHEISS and MCPHAIL (1989).

The Gamma Ray Attenuation Porosity Evaluation (GRAPE) measurements are based on the attenuation of gamma rays in marine sediments by Compton scattering (BOYCE 1976). The attenuation of gamma rays through the core is referred to the attenuation of aluminum standards. For calibration, two pieces of a PVC liner and 20 aluminum plates (5.3 mm thick) were each placed between the source and the detector. The expected theoretical attenuation can be calculated from the density data (about 2,7 g/ccm), the thickness of the aluminum plates and the count-rate measurement of gamma rays. During the measurement, a gamma ray beam of 0.662 MeV is emitted out from a hole (ϕ6 mm) and passes through the core. The 137Cs-source is shielded by a lead case. A scintillation detector (NaJ-crystal) measures the diminished radiation, which represents an indicator for wet bulk density. The physical principle of the Magnetic susceptibility meter is based on the magnetizability of atomic magnetic moments by external magnetic fields. A sensor loop with a diameter of 168 mm produces a weak, magnetic field. Interference with

magnetic sediment particles induces changes of the oscillation frequency of the electric circuit. These variations are detected and transformed into the magnetic susceptibility values that are given in SI-units. A detailed description of the GEOTEK Multi Sensor Core Logger and its use in sediment logging is given by CHI (1995).

Approximately 100 m of sediment cores were logged on board during M39/1. Prior to the measurement all cores were stored horizontally for 12 hours for thermal equilibration. During the cruise (sediment) temperatures varied between 16,6 and 21,2°C. Core liners were wetened with distilled water to ensure optimum acoustic coupling between the p-wave transducers and sediment cores. The drift of the susceptibility sensor was checked by measuring an iron ring that has a defined susceptibility signal.

Changes in acoustic and physical properties of marine sediments are closely related to the mean grain-size, bulk density, porosity, terrigenous material and percentage of sand, silt and clay. The p-wave velocity varies between 1450 m/s and 1500 m/s. In sections with a high amount of sandy components, the p-wave velocity increases up to 1600 m/s. Unrealistic high or low velocities (below 1450 or above 1600) were measured when coupling between p-wave transducer and the sediment was insufficient. In an ideal case there are no air-gaps between the liner and the sediment. But in practice the sediment does not fill the liner completely, having gaps mostly at the beginning and the end of a section. In this case the 500 kHz transducer signal is significantly weakened. Sediment gaps in the liners also distort the GRAPE measurements. For a satisfactory interpretation it would be necessary to correlate the p-wave velocity with the density data. In sections with a good correlation between compression-wave velocity and density, the physical properties can be used for interpretation of sedimentary processes. The density of marine sediments range between 1.45 and 1.9 g/ccm in the Gulf of Cadiz and at the Portuguese margin and, as expected, increases from top to bottom of these cores. Density variations on top of these general trend indicate changes of the mineralogical composition or of the water content. The magnetic susceptibility depends on the flux of terrigenous magnetic minerals. Generally susceptibility values are about 20 SI-units. In several cores prominent peaks up to 50 occur. Most magnetic susceptibility curves show a positive correlation with the curves of the p-wave-velocity and GRAPE-density.

b) PARASOUND and HYDROSWEEP Profiling in the Gulf of Cadiz

Due to good weather conditions and locally deep penetration high quality PARASOUND and HYDROSWEEP records from the Gulf of Cadiz were gained (Cadiz 4, Cadiz 5, Faro 1, Santa Maria 1, Santa Maria 2, Albufeira 1, Albufeira 2; Figure 55). Profile Cadiz 4 covers water depths from 700 m to 1100 m. Several pock marks were observed. These marks most frequently were V-shaped, either with or without levees (Figure 56). Vertically, they measure several meters, in cross sections up to one kilometer. The topography of the whole area is extremely rough. Profile Cadiz 5 covers 650 m to 1000 m water depths. The topography at the southern end of the survey box is extremely rough. This area is influenced by the tectonically active Gibraltar Fracture Zone. The other parts of the profile box has a smooth topography. The thickness of the stratified sequences in the smooth areas reaches up to 30 m and shows up to 12 reflectors. In the rough parts the penetration reaches up to 5 m, usually without subbottom reflectors.

Drift sediments in the northern Gulf of Cadiz were surveyed in three profiles. Profile Faro 1 covers the Faro Drift (Figure 57). The water depths ranges from 550 m in the North up to 800 m in the south and the profile lines were run N-S. The three-dimensional HYDROSWEEP Map shows the luv and the lee flanks of the sediment drift body. The penetration in the middle part of Faro drift body reaches up to 20 m, at the distal ends it is lower. The lines of Profile Santa Maria 1 and Santa Maria 2 were N-S oriented and show the sediment drift body east of profile Faro 1. The water depths ranged from 375 m in the north up to 950 in the south. At the northern end of the sediment drift body a channel like structure followed by a steep ascent occurred. The penetration in the middle part of the sediment drift body reaches up to 20 m, at both ends it is about 10 m. Profile Albufeira shows the east part of the sediment drift body in the Gulf of Cadiz. The lines of Profile Albufeira have a S-N orientation. The water depth decreases from about 350 m in the North to about 1000 m in the south. The penetration in the middle part of the sediment drift body reaches up to 25 m, at the distal ends about 10 m. At the northern end of the sediment drift body the channel structure of profiles S. Maria 1-2 reappeared. The sediment thickness of the drift body increase from E to W (profile Faro 1 to profile Albufeira).

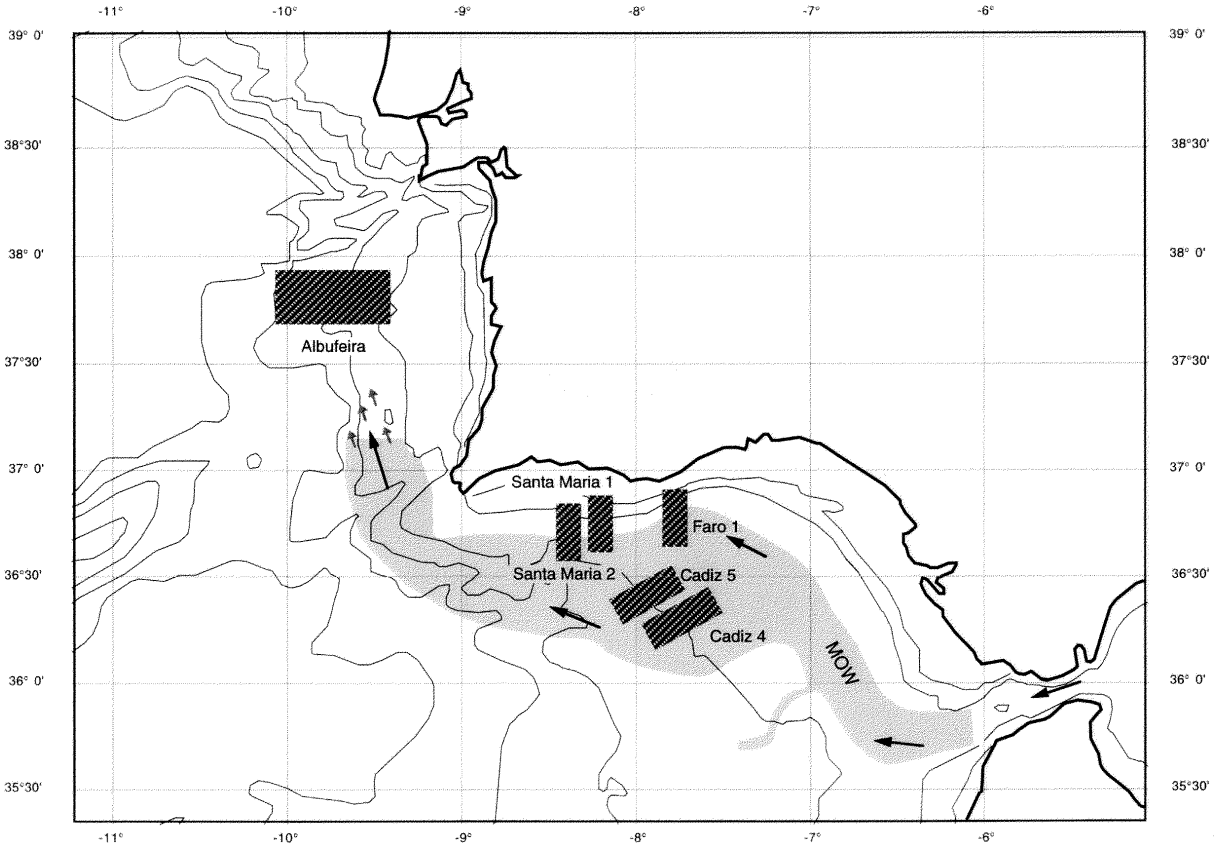

Figure 10: Location of acoustic survey boxes Cadiz 4, Cadiz 5, Faro 1, Santa Maria 1, Santa Maria 2, and Albufeira.

Fig. 55: Location of acoustic survey boxes Cadiz 4, Cadiz 5, Faro 1, Santa Maria 1, Santa Maria 2 and Albufeira.

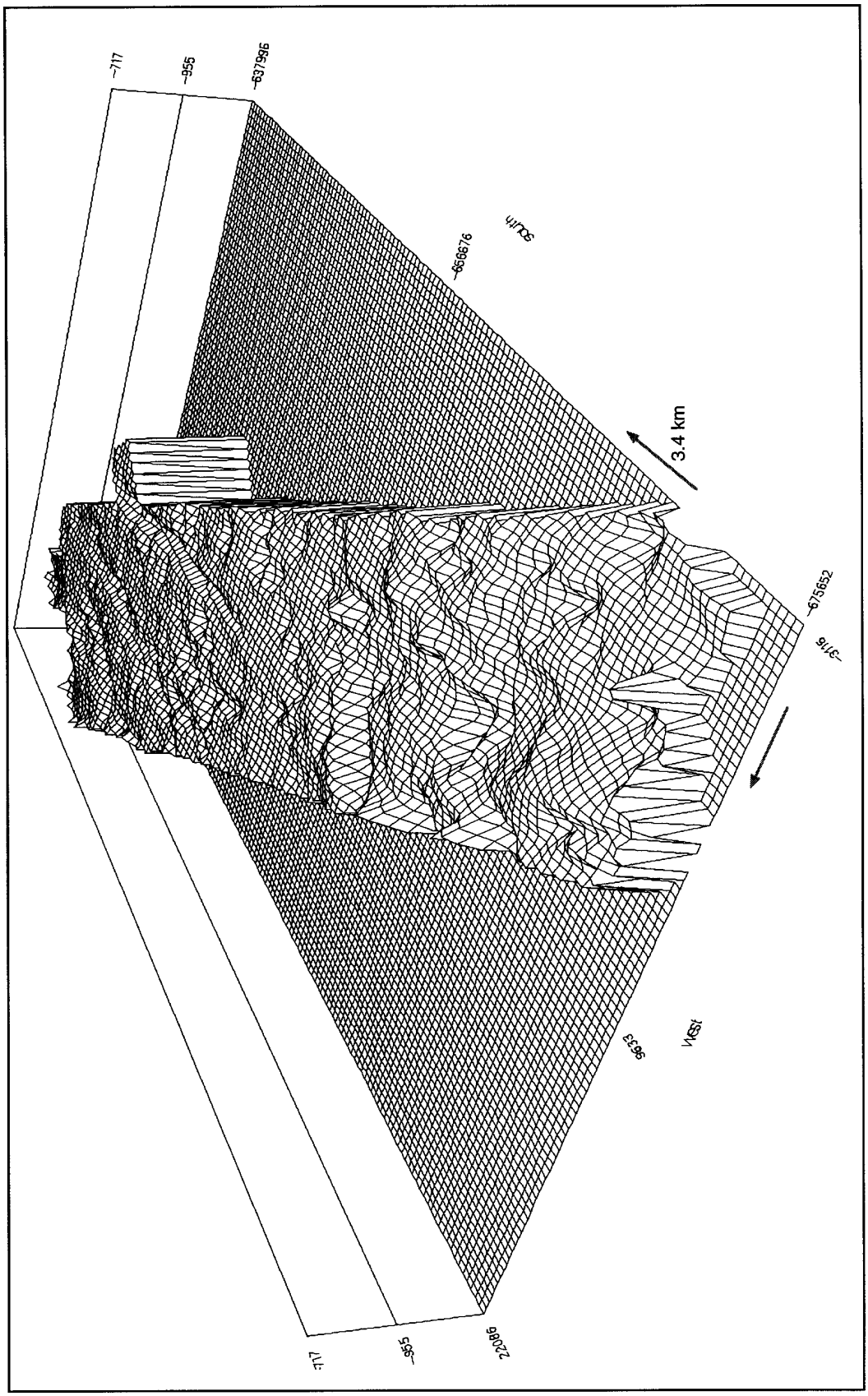

Fig. 56: Three dimensional HYDROSWEEP profile Cadiz 4. Water depths range from 760 m to 1140 m. Pock marks measure several meters in vertical direction and several hundreds of meters up to one kilometer in diameter.

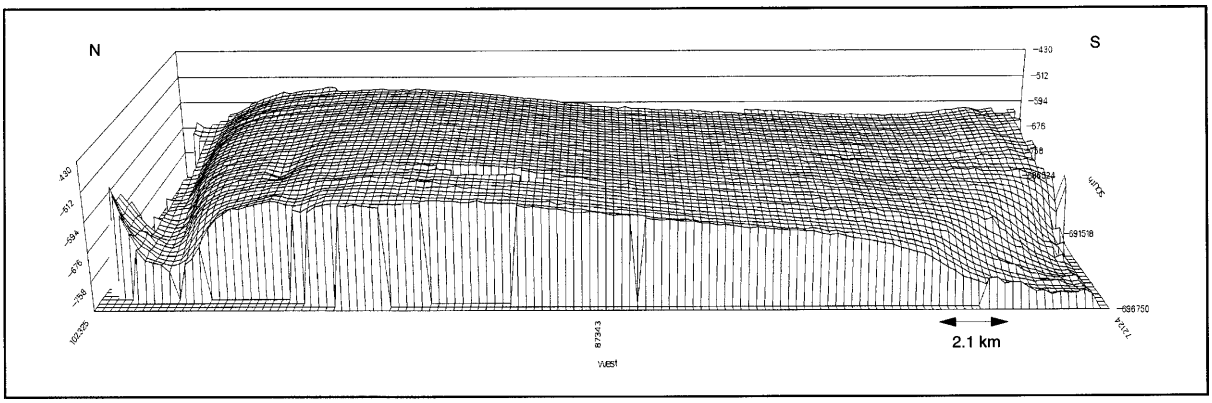

Fig. 57a: Three dimensional HYDROSWEEP profile Faro1. Shown are the luv and lee flanks of the sediment drift. Water depths range from 700 m to 1100 m.

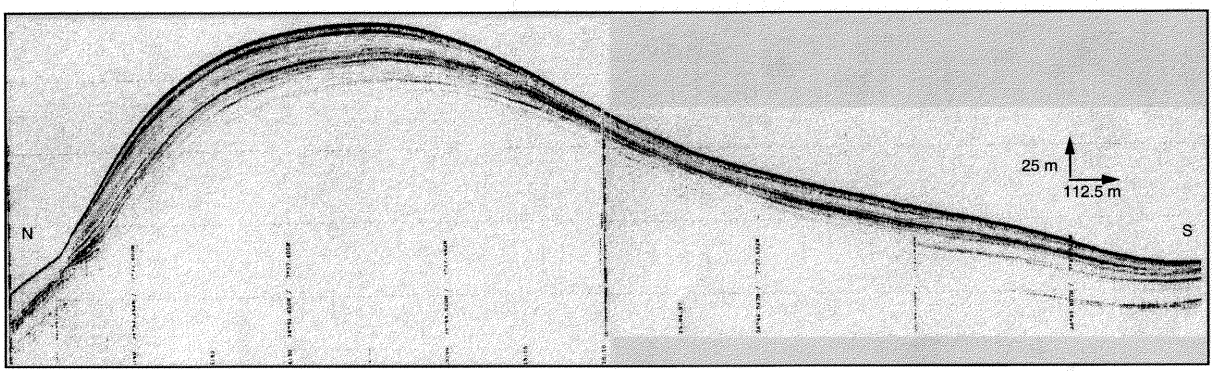

Fig. 57b: Stratified sequence of the luv and lee flank of a PARASOUND profile of the Faro Drift. Location: 36°53'N, 7°37'W/36°43'N, 7°37'W. Water depths range from 528 m in the north to 588 m in the south.

c) Core Logs as Indicators of Climate Change (S. Jung, R. Zahn)

Organic and inorganic composition as well as physical properties of deep sea sediments are controlled the ocean's physical circulation and chemical cycling. Carbonate dissolution, for instance, is driven by the state of carbonate saturation of ambient water masses which, in turn, is a function of carbon input and of chemical water mass "aging". Continuous high-resolution core logging is an indispensable tool for the evaluation of sediment composition and provides valuable data of fine-scale changes of sediment parameters that are intimately tied to state of ocean circulation and, ultimately, of global climate. Magnetic susceptibility logs and color scans of M39/1 sediment cores show numerous anomalies that can be correlated e.g., with horizons of enhanced concentration of terrigenous sediment components. Such horizons have been found previously in the northern North Atlantic and at the upper Portuguese margin and have been linked to periods of enhanced iceberg melting during the last glacial period (BOND et al., 1993; LEBREIRO et al., 1996; ZAHN et al., 1997). Figure 58 gives an example of the core logs that have been obtained during M39/1. The color scans show a series of positive reflectance excursions

that can be tentatively correlated to oxygen isotope anomalies in the GISP2 Greenland ice core record. The isotope anomalies signify short-lived warm (interstadial) episodes that are well know from continental European paleoclimate data bases and point to rapid climatic oscillations in the North Atlantic region (DANSGAARD et al., 1993; GROOTES et al., 1993; TAYLOR et al., 1993).

The apparent correlation between the color scan of core M39037-1 and the Greenland ice core record implies that the climate oscillations reached the western Iberian margin and conceivably affected climates of the western Mediterranean region. Planktonic isotope records that monitor surface ocean conditions will be generated for this core at the same resolution as the color scans i.e., at an average sample interval of 2 cm. This high-resolution isotope record will allow to test the predicted correlation with the ice core record as indicated in Figure 58. It will also allow to estimate the magnitude of environmental change at the western Iberian margin, far south of Greenland but reasonably close to the glacial position of the North Atlantic polar front at approximately 40°N. Statistical analysis of the planktonic foraminiferal assemblage will allow to estimate the variability of regional surface water temperature. The combined faunal and isotope data sets will help to better constrain the paleoceanographic patterns off Portugal and to determine the role of the Portugal current in transmitting northern North Atlantic climate signals as far south as Cape Blanc at 21°N off northwest Africa (WANG et al., 1995).

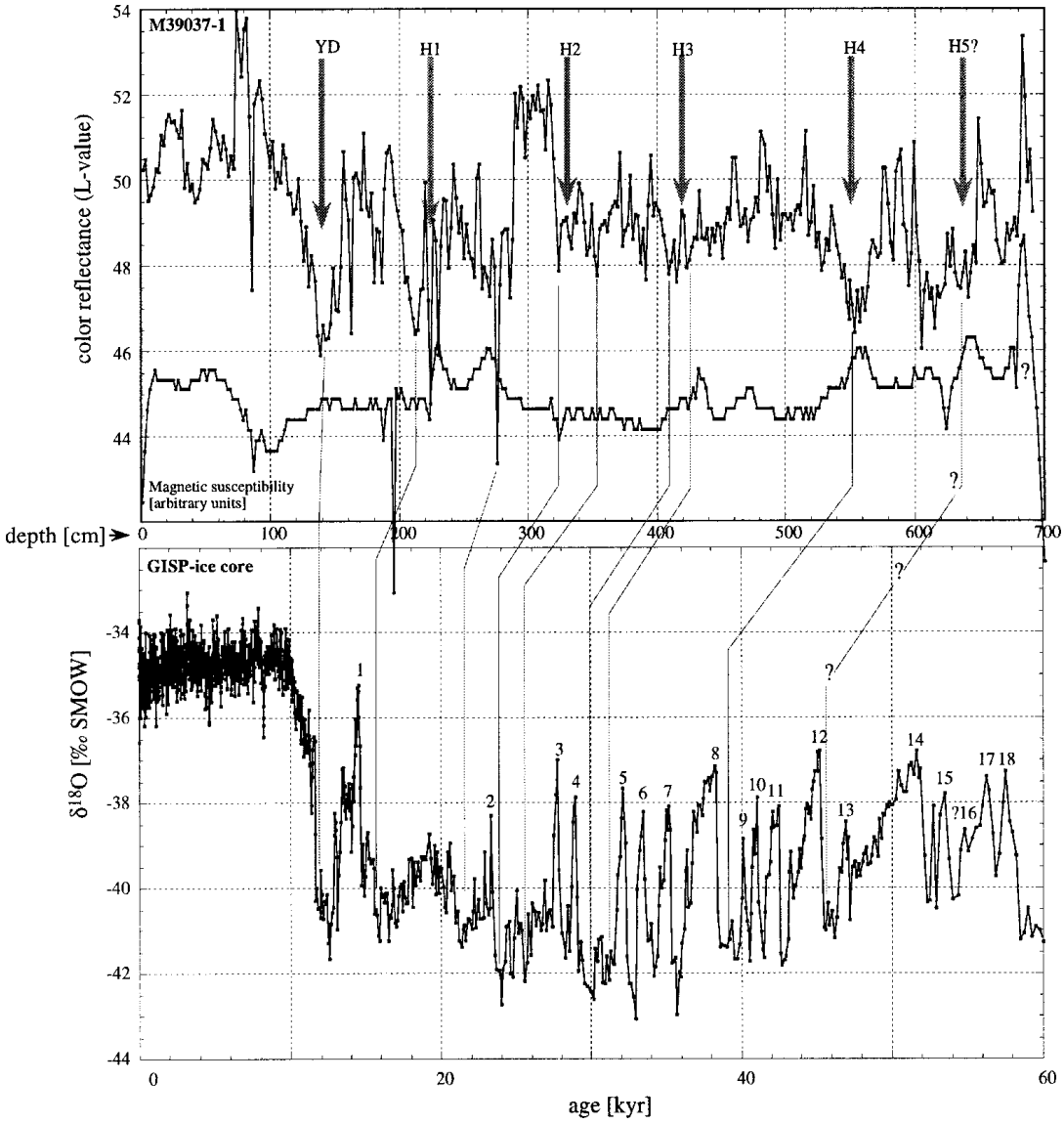

Fig. 58: Shipboard color reflectance and magnetic susceptibility logs for core M39037-1 from the western Iberian margin at 2533 m water depth (top). Arrows mark depth positions in the sediment core of 'Heinrich' meltwater events (labelled H1-H5) as predicted from reflectance minima and/or susceptibilty maxima. YD=Younger Dryas cold event. The Greenland GISP2 ice core oxygen isotope record is shown for refernce of northern North Atlantic climate variability (bottom). Prospective correlation between the GISP2 record and the M39037-1 color reflectance log is indicated and implies a close link between sediment property variations at the western Iberian margin and northern North Atlantic climate. Age scale along the ice core record is in 1000 years before present.